Investigating the Heliosphere with Low-energy Anomalous Cosmic Rays

Matthew E. Hill

Department of Physics, University of Maryland, College Park, MD 20742-4111

Abstract. Two aspects of low-energy ($\sim$0.5–30 MeV/nucleon) anomalous cosmic ray (ACR) phenomena are unique. First, low-rigidity ($\lesssim$ 2 GV) ACRs are less affected by particle drifts than higher rigidity particles [1]. Second, outer-heliospheric ACRs having energies below the energy at the peak of the modulated spectrum, but above the adiabatic range, are governed by a different limit of the transport equation than higher-energy ACRs, namely, the convection-diffusion limit [2, 3]. It is therefore possible to uncover features of energetic particle transport in the heliosphere that are not readily apprehended using higher-energy ACR measurements [e.g., 4]. We study the first property, in the context of outer-heliospheric Voyager 1 (V1), Voyager 2 (V2), and Pioneer 10 (P10) particle intensity measurements made during the 1991-1999 cosmic ray recovery phase. In particular, we show that the effective "drift/convection pattern" of low-rigidity particles during a period of positive heliomagnetic polarity ($A > 0$), such as this, is qualitatively different than the drift pattern usually discussed. The disagreement between radial and latitudinal intensity gradients determined using the new "quasi-local" gradient (QLG) method [5, 6] and the standard non-local gradient (NLG) method [7] is discussed in light of models of the heliosphere showing longitudinal asymmetry [8]. Earlier results regarding diminished high-latitude transport [9–12] suggest that the near-equatorial region will have an enhanced role in the ACR transport. Absent this effect, the fact that the detected low energy particles are actually cooled products of higher energy populations would lead to the expectation that the cooled particles should show residual evidence of the drift undergone before the energy loss took place. The lack of such evidence suggests low latitudes are the more significant region. We will discuss these topics with the primary goal of highlighting the unique and necessary role low-energy ACR measurements have in studying the heliosphere.

1. DRIFT VELOCITY

Influences on the transport of charged particles in the heliosphere include convection and energy loss due to the solar wind flow and divergence and diffusion due to particles scattering off of irregularities in the magnetic field suffusing the heliosphere. The process most recently understood to be important is particle drift [1], a fundamental effect of curvature and gradients in magnetic fields. Although widely studied, observational tests of drift-diffusion theory have concentrated on high-energy particles (> 10 MeV/nuc) and observations close to the Sun (< 5 AU). Because much of the intuition regarding ACR transport has been gained through the study of particles having a rigidity $R > 2$ GV, it is important to highlight the unique lower-rigidity phenomena and disabuse ourselves of notions that may be inappropriately applied at low-rigidities.

Before simplifying the equation of Jokipii et al. [Ref. 1, Eq. 6] for the drift velocity $\mathbf{v}_D$ in the heliosphere with a constant solar wind speed and a flat neutral current sheet—a flat geometry is a significant approximation, more appropriate at solar minimum—we indicate that m, u, and q are the particle mass, speed, and charge, r, λ, and φ are the

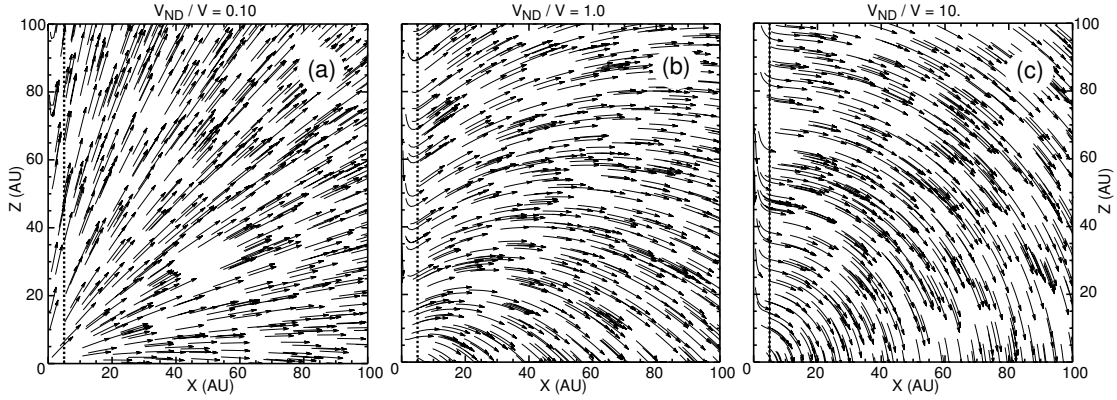**FIGURE 1.** Streamlines of vectorially added drift and solar wind velocities in the heliosphere for $\frac{v_{ND}}{V} = 0.1$, 1.0, and 10., from left to right, for a constant radial solar wind speed. The Sun is at the origin, the ordinate is the heliographic Z axis, North of the solar pole, and the abscissa is the orthogonal dimension X in the heliographic equatorial plane, with a 100 AU scale. The vertical dotted line describes a cylinder coaxial with the solar rotation axis that defines the inner boundary of the region of applicability for the "outer heliospheric" approximation; i.e., $X = r\cos\lambda \gg 1$ AU. At low rigidities (see Table 1), (a) the drift speed is negligable and the solar wind dominates, while at higher rigidities, (c) the drifts are dominant and the familiar $A > 0$ drift pattern can be seen.

heliographic radius, latitude, and longitude ("hats" designate unit vectors), Ω and V are the solar rotation rate and solar wind speed, and A and c are a constant (defined below) and the speed of light, respectively. We use $R = muc/q$ and make the simplifying assumption, $\frac{r\Omega}{V}\cos\lambda \gg 1$, which can be written $r\cos\lambda \gg \frac{V}{\Omega} \approx 1\text{AU} \equiv r_o$, for a nominal solar rotation rate and solar wind speed of $14 \times 2\pi/\text{year}$ and 85 AU/year (400 km/s), respectively. This describes the large region outside of a small cylindrical volume (with a radius of, say, ~ 5 AU) coaxial with the Sun's spin axis; i.e., everywhere except the inner heliosphere and the extreme polar regions (Figure 1). The magnetic field is given by $\mathbf{B} = A\left(\hat{r}/r^2 - \hat{\varphi}\Omega\cos\lambda/Vr\right)$ [1], which in the outer heliospheric approximation provides a relationship $B = A\Omega\cos\lambda/Vr$ between A and the field strength B. Hence, an approximate form for the drift velocity (for $\lambda \neq 0$ and $A > 0$) is,

$$\mathbf{v}_D \approx \frac{2}{3}u\frac{\rho}{r}\left[-\frac{V^2}{r^2\Omega^2}\frac{\sin\lambda}{\cos^3\lambda}\hat{r} - \hat{\lambda} + \frac{V}{r\Omega}\frac{\sin\lambda}{\cos^2\lambda}\hat{\varphi}\right] \equiv -v_{Dr}\hat{r} - v_{D\lambda}\hat{\lambda} + v_{D\varphi}\hat{\varphi}, \quad (1)$$

where $\rho = R/B$ is the particle gyroradius ($\rho = R/Bc$ in SI units). The magnitude v_{ND} of the outer heliospheric drift speed along a flat current sheet (for $\lambda = 0$, where $\mathbf{v}_D \approx v_{ND}\hat{r}$) provides a convenient scale with which to write the components of the drift velocity:

$$v_{Dr} = v_{ND}\frac{r_o^2}{r^2}\frac{\sin\lambda}{\cos^3\lambda}, \quad v_{D\lambda} = v_{ND}, \quad v_{D\varphi} = v_{ND}\frac{r_o}{r}\frac{\sin\lambda}{\cos^2\lambda}, \quad \text{and} \quad v_{ND} \equiv \frac{2}{3}u\frac{\rho}{r}.$$

Equation (1) is used to calculate the direction of the vector sum of the drift and convection velocities at points in the XZ-plane, for $v_{ND}/V = 0.1$, 1.0, and 10.0 (Figure 1). Now, we can easily compare the drift scale v_{ND} to the solar wind speed for various ACRs to estimate where drifts are significant contributors to their transport. A convenient form for the gyroradius is $\rho = \frac{2}{9}10^{-4}\text{AU}(R/\text{MV})/(B/\text{nT})$ and we can write

TABLE 1. Drift speeds and intensity gradients of anomalous cosmic rays.

Ion[*]	$E^\dagger$ (MeV/nuc)	R (MV)	v_{ND} (km/s)	$\frac{v_{ND}}{V}$ **	ref.[‡]	g_r (%/AU)	g_λ (%/°)	α_r §	α_λ ¶
H	24-30	224	108	0.27	[5]	16 ± 3	-10 ± 2	–	–
H	30-56	277	164	0.41	[7]	3.0 ± 0.2	0.6 ± 0.2	1.66 ± 0.05	1.62 ± 0.04
He	3-12	424	96	0.24	[5]	13.3 ± 1.6	-7.5 ± 1.6	–	–
He	6-10	482	124	0.31	[7]	3.7 ± 0.3	1.9 ± 0.3	1.54 ± 0.04	1.55 ± 0.04
He	21-30	868	400	1.00	[5]	8.1 ± 1.3	-3.9 ± 1.6	–	–
He	30-56	1109	656	1.64	[7]	1.7 ± 0.3	1.1 ± 0.2	1.63 ± 0.04	1.59 ± 0.07
O	7-28	2592	896	2.24	[5]	0.9 ± 0.9	2.8 ± 0.8	–	–
O	8-18	2400	768	1.92	[7]	1.9 ± 0.6	0.2 ± 0.6	–	–

[*] assumed to be singly ionized
† kinetic energy per nucleon
** for nominal solar wind speed $V = 85$ AU/yr $= 400$ km/s
‡ reference for gradient measurement: V1-V2-P10, 1996, NLG [7]; V1-V2, 1994-1999, QLG [5, 6]
§ tailward scaling factor for radial gradient (this work, see Section 2)
¶ tailward scaling factor for latitudinal gradient (this work, see Section 2)

the magnetic field strength as $B = (2.2 \, \text{nT} \cos \lambda)/(r/r_o)$, based on the measurement at Voyager 1 in 1996 of a 0.03 nT field at 62 AU and 33° [13]. In combination we get the drift scale in terms of total kinetic energy $\mathscr{T}$ and charge ($q = z$e; $z \neq$ atomic no.), $v_{ND} = z^{-1}(0.85 \text{AU/yr})(\mathscr{T}/\text{MeV}) = z^{-1}(4 \text{ km/s})(\mathscr{T}/\text{MeV})$, which is applied in Table 1 to compare the drift and solar wind speeds for ACRs of various rigidities.

2. INTENSITY GRADIENTS

There is observational evidence that transport of low-rigidity ($R \lesssim 2$ MV) ACRs is not significantly influenced by drift effects. Latitudinal intensity gradients g_λ were determined using a "quasi-local" gradient (QLG) method [5, 6, 14] and it was found that the gradients were negative for ions—measured at V1 & V2 from 1994 to 1999—with rigidities below ~ 2 GV. This finding was unexpected, since during the prevailing heliospheric polarity at the time ($A > 0$), the expectation was that latitudinal intensity gradients would be positive. The expectation was confirmed for higher-energy ACRs [e.g., Ref. 7] although the magnitudes of the gradients were smaller than the prediction of the original drift-diffusion transport theory [15, and references therein] before later theoretical developments [9] and results from the Ulysses mission out of the ecliptic plane [10–12] modified this expectation. This change is primarily due to turbulent, non-Archimedean fields impeding the sunward, radial diffusion and drift of cosmic rays above the solar poles [9, 11]. From section 1 and Table 1 it can be seen that the negative latitudinal gradients occur for $v_{ND} \lesssim V$. In addition to the non-Archimedean field effects a possible explanation for the negative latitudinal gradients is the influence of high speed solar wind at high latitudes, which would act to reduce inward transport of ACRs at high latitudes.

Table 1 shows that at higher rigidities ($R > 2$ GV) there is substantial agreement

between the results of the QLG and non-local gradient (NLG) methods [see Ref. 5, for an extensive table]. However below 2 GV there is a large disagreement between the results of these methods, e.g., NLG has positive and QLG negative latitudinal gradients. The NLG method is the traditional three-spacecraft method used to algebraically determine two simultaneous intensity gradients from three separate intensity observations. Both methods start with the relation $dj = (\partial j/\partial r)dr + (\partial j/\partial \lambda)d\lambda$ for the differential of intensity j as a function of r and λ. The NLG method uses the integration of this relation between three positions to get a system of equations,

$$\begin{aligned}
\ln(j_1/j_2) &= g_r(r_1 - r_2) + g_\lambda(\lambda_1 - \lambda_2) \\
\ln(j_2/j_\circ) &= g_r(r_2 - r_\circ) + g_\lambda(\lambda_2 - \lambda_\circ),
\end{aligned} \tag{2}$$

which is solved for $g_r \equiv \frac{\partial \ln j}{\partial r}$ and $g_\lambda \equiv \frac{\partial \ln j}{\partial \lambda}$. The QLG method begins with the same equation for dj to get $y_{mn} = g_r + x_{mn}g_\lambda$, with $y_{mn} \equiv \ln(j_m/j_n)/(r_m - r_n)$ and $x_{mn} \equiv (\lambda_m - \lambda_2)(r_m - r_n)$. The set of data-points (x_{mn}, y_{mn}) is determined empirically for all unique pairs mn of observations during a specified time period, a linear fit to which determines g_r and g_λ. The temporal resolution of the NLG method is limited only by the data cadence, but NLG is restricted in spatial resolution by the non-locality of the simultaneous spatially separated observations. The spatial resolution of the QLG method is *quasi-local* since the separation between observation points (e.g., along a single spacecraft trajectory) is specified by the data cadence, but QLG is restricted in temporal resolution, requiring a period long enough to provide a sufficient number of (x_{mn}, y_{mn}) data points to which a fit can be made. Since the QLG method can use fewer spacecraft, the spatial assumptions required are less extensive than with the NLG method. In this case the QLG values are determined from measurements from V1 and V2, which are both roughly in the apex direction (the direction of relative motion of the heliosphere with respect to the local interstellar medium), minimizing the possibility of effects due to longitudinal asymmetry. In addition to these spacecraft, however, the NLG method require the use of P10, which is positioned near the equatorial plane, but in the anti-apex or tailward direction. This means that these NLG values are more sensitive to longitudinal asymmetry than are the QLG values. (Analogously, the QLG method is more sensitive to temporal assumptions.) The details of the similarities and differences of these two methods, including a complete description of the QLG procedure, appear elsewhere [5, 6, 14], but here the issue of longitudinal asymmetry is addressed.

Global models of the heliosphere [8] suggest that the distance between the Sun and ACR source at the termination shock (TS)[16] in the anti-apex direction may be larger than this distance in the apex direction, perhaps by a factor of ~ 2. Since P10 is conveniently located very near the equator, in the anti-apex direction, a simple calculation determines the effect on gradients of a heliosphere stretched in the tailward direction. The set of equations (2) is modified by replacing the P10 radius $r_\circ$ with the effective radius for P10 under the condition of the assumed tailward scaling of the heliosphere by a factor α, i.e., $r_\circ \to r'_\circ = r_\circ/\alpha$. Figure 2 shows the change in the radial and latitudinal gradient as α varies from zero to two for the example of ~ 7 MeV/nuc He. The NLG values—which were calculated under the assumption of longitudinal symmetry—are indicated in each panel of Figure 2 where the modified gradient curve crosses $\alpha = 1$. The value of α coinciding with the QLG value associated with this energy
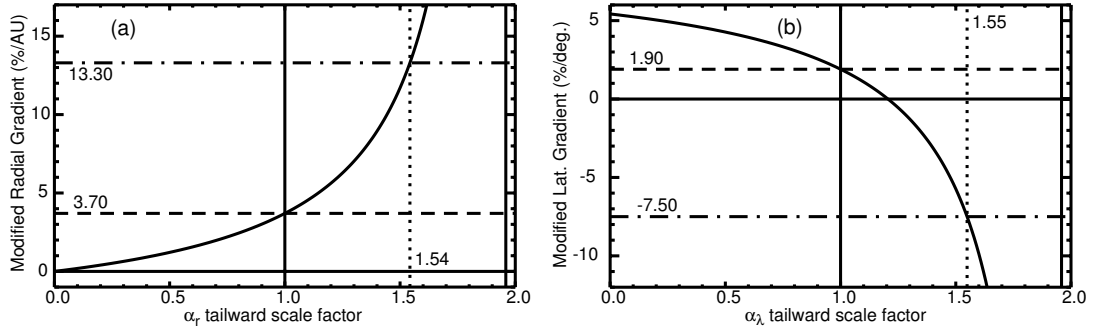
FIGURE 2. Example of the effect on V1-V2-P10 ACR intensity gradients of scaling the heliosphere in the tailward direction for ~7 MeV/nuc He. Radial (a) and latitudinal (b) intensity gradients are plotted versus a scaling factor α which specifies the asymmetry in the heliospheric length scale (~Sun-TS distance) as an anti-apex to apex ratio (see Section 2). In each panel the horizontal dashed line indicates the gradient value determined with the 3-spacecraft, non-local gradient method with longitudinal symmetry assumed [7] and the horizontal dash-dot line indicates the gradient value determined with the 2-spacecraft, quasi-local gradient method [5, 6]. The solid curve shows the modification in the gradient as a function of the tailward scaling factor. The vertical dotted line indicates the magnitude of the tailward "stretching" required to bring the NLG value into agreement with the QLG value. As indicated in Table 1 all six low-rigidity gradients are independently brought into agreement with a ~60% asymmetry.

range is indicated in each panel. The six resulting scale factors calculated for the $R < 2$ GV gradients are listed in Table 1 and are all in agreement, indicating a scaling factor $\alpha \approx 1.6$. The fact that this calculation yields consistent scale factors is suggestive that this value may have a direct physical significance and we note that a 60% extension in the tailward direction appears to be well within the range of heliospheric models [e.g., 8]. The simplicity of this estimate, however, should warn against over-interpretation of the result; it is clear that a more sophisticated examination of this issue is desirable.

3. DISCUSSION

The fact that a scaling in the equatorial region has brought the NLG values into agreement with the QLG values has implications involving the pattern of the drift velocity and the inhibition of ACR transport at higher latitudes. This is consistent with the interpretation that lower-latitude transport is more important during $A > 0$, as discussed by Van Allen [15]. Moreover it supports the conception indicated by the negative latitudinal gradient measurements that drifts are not significant for ACRs having rigidities below ~2 GV. If it were the case that drifts were dominant at these low rigidities then the primary direction of transport would be from over the poles toward the equatorial regions as shown in Figure 1c. If this were so, then it would not be expected that a scaling in the equatorial plane, such as that in Section 2, would have a significant effect on the gradient measurements. Another issue is the expectation that the low-energy particles detected are expected to have begun their transport at higher energies and then to have cooled during the process of transport. If there were a significant population of higher energy ACRs strongly drifting down from high latitudes, the expectation is that

the influence of this drift on these particles (detected after having undergone significant energy loss) would be in evidence. That the gradient measurements show no evidence of significant drift for $R \lesssim 2$ GV particles (i.e., convection is more important) suggests that this more energetic population is not predominantly drifting in this way (the necessary quantitative analysis of this conjecture has yet to be performed). This is reasonable if the high-latitude inhibition is a strong effect, limiting the access of a high latitude source of ACRs. This suggests the interpretation in which the high latitudes play a small role, leaving the low-latitude region as the primary transport region. Therefore the transport of ACRs at these latitudes will be largely radial since the most important source is not at high latitudes. This would also explain why spherically symmetric numerical modeling of the transport of ACRs during this $A > 0$ period are surprisingly successful in matching the observed modulated spectra throughout the heliosphere [5, 17].

In summary, we emphasized that the well-known $A > 0$ drift pattern (i.e., Figure 1c) does not apply for $R \lesssim 2$ GV. We discussed the non-local and quasi-local intensity gradient methods, which disagree at low-rigidities, and undertook a simple model to address a possible apex-to-tail asymmetry in the heliosphere. A heliosphere stretched in the tailward direction by 60% brings all six NLG values into agreement with the QLG values (Table 1). In addition, a consistent interpretation of outer heliospheric ACR transport during the 1991-1999 $A > 0$ period emerges in which (1) high-latitude transport is suppressed; (2) drifts are weak at all rigidities and negligible for $R \lesssim 2$ GV; (3) low-rigidity ACRs transport in a nearly radial (drift-free) manner; (4) negative latitudinal gradients at low-rigidity may be caused by high-latitude, high-speed wind or the inhibited transport due to polar magnetic field effects; and (5) high-rigidty ACRs do originate and drift down from somewhat higher latitudes.

REFERENCES

1. J.R. Jokipii, E.H. Levy, and W.B. Hubbard, Astrophys. J. **213**, 861-868, 1977.
2. J.P.L. Reinecke and H. Moraal, Astrophys. J. **392**, 272-276, 1992.
3. R.A. Caballero-Lopez and H. Moraal, J. Geophys. Res **109**, A01101, doi:10.1029/2003JA010098, 2004.
4. A.C. Cummings, E.C. Stone, and C.D. Steenberg, Astrophys. J. **578**, 194-210, 2002.
5. M.E. Hill, Ph.D. Thesis, Univ. Maryland, College Park, 2001.
6. M.E. Hill and D.C. Hamilton, Proc. 28th Int. Cosmic Ray Conf. (Tsukuba) **7**, 3969-3972, 2003.
7. F.B. McDonald, N. Lal, and R.E. McGuire, J. Geophys. Res. **103**, 373-379, 1998.
8. G.P. Zank and H.-R. Müller, J. Geophys. Res. **108**, 1240, doi:10.1029/2002JA009689, 2003.
9. J.R. Jokipii and J. Kota, Geophys. Res. Letters **16**, 1-4, 1989.
10. R.J. Forsyth, A. Balogh, E.J. Smith, N. Murphy, and D.J. McComas, Geophys. Res. Letters **22**, 3321-3324, 1995.
11. J.R. Jokipii, J. Kota, J. Giacalone, T.S. Hornbury, and E.J. Smith, Geophys. Res. Letters**22**, 3385-3388, 1995.
12. R.J. Forsyth, A. Balogh, E.J. Smith, G. Erdös, and D.J. McComas, J. Geophys. Res. **101**, 395-403, 1996.
13. N.F. Ness and L.F. Burlaga, J. Geophys. Res. **106**, 15 803-15 817, 2001.
14. M.E. Hill, in preparation, 2004.
15. J.A. Van Allen, Geophys. Res. Letters **27**, 2453-2456, 2000.
16. M.E. Pesses, J.R. Jokipii, and D. Eichler, Astrophys. J. **246**, L85-L88, 1981.
17. C.D. Steenberg, Ph.D. Thesis, Potchefstroom Univ., South Africa, 1998.